

# Mechanism of Formation of Two-Dimensional Crystals from Latex Particles on Substrates

N. D. Denkov,<sup>†</sup> O. D. Velev,<sup>†</sup> P. A. Kralchevsky,<sup>†</sup> I. B. Ivanov,<sup>\*,†</sup>  
H. Yoshimura,<sup>‡</sup> and K. Nagayama<sup>‡</sup>

Laboratory of Thermodynamics and Physico-chemical Hydrodynamics, Faculty of Chemistry,  
University of Sofia, 1126 Sofia, Bulgaria, and Protein Array Project, ERATO, JRDC,  
18 - 1 Higashiarai, Tsukuba 305, Japan

Received April 14, 1992. In Final Form: October 6, 1992

The dynamics of two-dimensional ordering of micrometer-size polystyrene latex spheres on a horizontal glass substrate has been directly observed by means of optical microscopy. It turns out that the ordering starts when the thickness of the water layer containing particles becomes approximately equal to the particle diameter. By variation of the electrolyte concentration, the charge of the particles, and their volume fraction, it is proven that neither the electrostatic repulsion nor the van der Waals attraction between the particles is responsible for the formation of two-dimensional crystals. The direct observations revealed the main factors governing the ordering—the attractive capillary forces (due to the menisci formed around the particles) and the convective transport of particles toward the ordered region. The control of the water evaporation rate turns out to allow obtaining either well-ordered monolayers or well-ordered domains consisting of multilayers (bilayers, trilayers, etc.).

## 1. Introduction

In his classical works on determining the Avogadro number Perrin<sup>1</sup> measured the size of submicrometer particles by forming a two-dimensional (2D) array of particles on a solid substrate. For that purpose he used a suspension containing monodisperse spherical particles of gomme-gutte. Some amount of this suspension was deposited on a glass plate and observed by a microscope. In some cases Perrin observed formation of ordered 2D aggregates; see Figure 1, which is Perrin's original photograph. As far as we know, this is the first description of 2D array formation from colloid particles in the scientific literature.

The more recent works of Pieranski et al.<sup>2,3</sup> and Van Winkle and Murray<sup>4,5</sup> deal with charged latex particles confined between two smooth glass surfaces at a distance comparable with the particle diameter. As claimed by these researchers, the electrostatic interactions play a dominant role in these systems, which in fact represent two-dimensional counterparts of the 3D crystals from charged spherical particles.<sup>6-13</sup> On the other hand, formation of two-dimensional colloid crystals of a different kind was recently reported<sup>14-17</sup> where just as in the experiments of Perrin,<sup>1</sup> the particles (protein molecules or latex spheres) have been initially suspended in a liquid

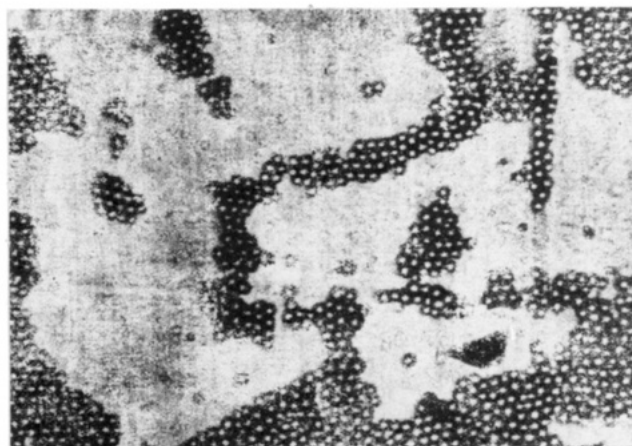


Figure 1. Two-dimensional ordered clusters from colloidal particles observed by J. Perrin.<sup>1</sup> Reprinted with permission from ref 1. Copyright 1909 Masson.

drop which spreads on a horizontal flat surface (substrate). After the evaporation of the solvent, well-ordered two-dimensional arrays from hexagonally packed particles have been observed by means of electron microscopy<sup>14,15</sup> and scanning tunneling microscopy.<sup>16</sup> The good quality of the 2D protein arrays obtained on a mercury substrate<sup>14,15</sup> allowed investigating the protein structure and orientation by using diffraction image reconstruction. The two-dimensional arrays, which can be obtained in a reproducible and controllable way, can find application as new materials in some modern industries, e.g., in optical units,<sup>17-19</sup> data storage, microelectronics, and others.

The experimental studies of both protein<sup>14-16</sup> and polystyrene<sup>17</sup> 2D arrays, represent observations of the final result of ordering. However, the mechanism and stages of the process of ordering have not been investigated in

\* To whom correspondence should be addressed.

<sup>†</sup> University of Sofia.

<sup>‡</sup> JRDC.

(1) Perrin, J. *Ann. Chim. Phys.* **1909**, *18*, 1.

(2) Pieranski, P.; Strzelecki, L.; Pansu, B. *Phys. Rev. Lett.* **1983**, *50*, 900.

(3) Pansu, B.; Pieranski, P. *J. Phys.* **1984**, *45*, 331.

(4) Van Winkle, D. H.; Murray, C. A. *Phys. Rev. A* **1986**, *34*, 562.

(5) Murray, C. A.; Van Winkle, D. H. *Phys. Rev. Lett.* **1987**, *58*, 1200.

(6) Pieranski, P. *Contemp. Phys.* **1983**, *24*, 25.

(7) van Megen, W.; Snook, I. *Adv. Colloid Interface Sci.* **1984**, *21*, 119.

(8) Castillo, C. A.; Rajagopalan, R.; Hirtzel, C. S. *Rev. Chem. Eng.* **1984**, *2*, 237.

(9) Russel, W. B. *Dynamics of Colloidal Systems*; University of Wisconsin Press: Madison, 1987.

(10) Efremov, I. E. In *Surface and Colloid Science*; Matijevic, E., Ed.; Wiley: New York, 1978; Vol. 8, p 71.

(11) Russel, W. B.; Saville, D. A.; Schowalter, W. R. *Colloidal Dispersions*; Cambridge University Press: Cambridge, 1989.

(12) Hachisu, S.; Kobayashi, Y.; Kose, A. *J. Colloid Interface Sci.* **1973**, *46*, 342.

(13) Furusawa, K.; Tomotsu, N. *J. Colloid Interface Sci.* **1983**, *93*, 504.

(14) Yoshimura, H.; Endo, S.; Matsumoto, M.; Nagayama, K.; Kagawa, Y. *J. Biochem.* **1989**, *106*, 958.

(15) Yoshimura, H.; Matsumoto, M.; Endo, S.; Nagayama, K. *Ultra-microscopy* **1990**, *32*, 265.

(16) Haggerty, L.; Watson, B. A.; Barteau, M. A.; Lenhoff, A. M. *J. Vac. Sci. Technol., B* **1991**, *9*, 1219.

(17) Hayashi, S.; Kumamoto, Y.; Suzuki, T.; Hirai, T. *J. Colloid Interface Sci.* **1991**, *144*, 538.

(18) Deckman, H. W.; Dunsmuir, J. H. *Appl. Phys. Lett.* **1982**, *41*, 337.

(19) Deckman, H. W.; Dunsmuir, J. H.; Garoff, S.; McHenry, J. A.; Peiffer, D. G. *J. Vac. Sci. Technol., B* **1988**, *6*, 333.

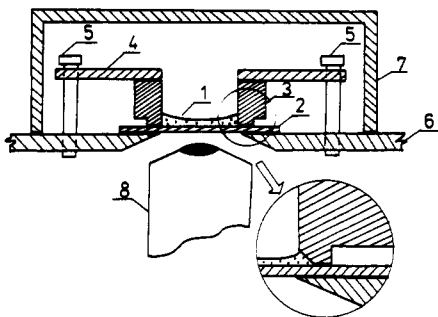


**Figure 2.** Scheme of the basic experimental cell: (1) latex suspension, (2) glass plate, (3) Teflon ring, (4) brass plate, (5) screws, (6) microscope table, (7) glass cap, (8) microscope objective.

these studies, which does not permit definite conclusions about the forces governing the ordering.

In this study we report experimental results revealing the mechanism of array formation from micrometer-size latex particles on glass substrata. For this purpose an experimental cell is designed which allows direct microscopic observations and control of the ordering processes (see section 2 below). An outline of the observed phenomena is given in section 3.1. The roles of different factors (particle size and concentration, presence of electrolytes, water evaporation rate, etc.) are discussed in section 3.2. An analysis of the proposed mechanism of 2D array formation is presented in section 3.3. Section 3.4 deals with the results concerning the controllable formation of bi-, tri-, and multilayer arrays. The results and conclusions are summarized in section 4.

## 2. Experimental Section

**2.1. Investigated Systems.** Most of the experiments were carried out with a 1 wt % suspension of polystyrene latex (JSR, Stadex, Japan) with a particle diameter of 1.70  $\mu\text{m}$ . The measurements of the surface electric  $\zeta$ -potential of the particles (by means of a Zetasizer IIC, Malvern Instruments Ltd., England) showed that they are strongly charged:  $\zeta = -106 \pm 2$  mV with 0.01 M added NaCl at 25  $^{\circ}\text{C}$ .

In one set of experiments a latex with a smaller particle diameter and the same concentration was used: 0.814  $\mu\text{m}$  (JSR, Stadex, Japan). The measured  $\zeta$ -potential was  $\zeta = -90 \pm 2$  mV under the same experimental conditions (0.01 M NaCl at 25  $^{\circ}\text{C}$ ). The two latex suspensions were used without additional purification.

In some experiments the suspensions were diluted by adding water purified by a Milli-Q Organex system (Millipore, MA). NaCl (Merck) was heated for several hours at 500  $^{\circ}\text{C}$  before use to remove the humidity and organic impurities. The surfactants sodium dodecyl sulfate (Fisher Scientific) and hexadecyltrimethylammonium bromide (Sigma) were used without additional purification.

As substrates we used hydrophilic microscope cover glass plates (Ilmglas, Germany) with a thickness of 0.17 mm. The glass plates and the Teflon rings were thoroughly cleansed by washing them with detergent, with subsequent immersion for more than 24 h in chromic acid, followed by abundant washing with deionized water from the Milli-Q Organex system. The cleaned plates were kept under deionized water from 6 to 12 h and vacuum dried just before the experiment.

**2.2. Experimental Cell and Procedure.** The setup shown in Figure 2 was used in most of the experiments. A drop of the latex suspension (1 in Figure 2) with a given volume and composition is placed upon the glass plate (2). The drop spreads over the accessible glass area encircled by a Teflon ring with an inner diameter of 14 mm (3 in Figure 2). The ring is pressed against the glass (to avoid leakage of the liquid) by a brass plate (4) and screws (5). The system is mounted on the table (6) of a metallographic microscope and is covered by a glass cover (7) which allows illumination from above. The observations are

performed through the bottom in reflected monochromatic light (wavelength  $\lambda_0 = 546$  nm) or transmitted polychromatic light. Objectives (8) with magnification from  $\times 4$  to  $\times 100$  (the latter one being of the immersion type) were used.

In another set of experiments an improved version of the cell was used which allows control of the water evaporation rate (by variation of the temperature of the upper glass cover) as well as of the volume of the liquid inside the cell during the ordering process; see section 3.4.

## 3. Experimental Results and Discussion

**3.1. Dynamics of the Ordering Process.** We start with a phenomenological description of the main stages of the ordering process with a pure latex suspension as observed in the cell shown in Figure 2. The mechanism of ordering and the forces governing it are discussed in detail in section 3.3 below. Initially, a 20- $\mu\text{L}$  drop of the suspension is spread over the bottom of the experimental cell. The volume and the concentration of the spread amount of suspension were chosen to provide (approximately) the formation of a dense monolayer of particles after the evaporation of water. The drop spontaneously spreads and forms a slightly concave layer (Figure 2), whose thickness is about 100  $\mu\text{m}$  at the center of the cell. The microscopic observations show that the latex particles in this layer are involved in intensive Brownian motion. Initially their concentration just above the glass surface is comparatively low. Several minutes after the beginning of the experiment one can see that the particle concentration in close vicinity to the glass surface becomes higher than in the bulk of the aqueous layer due to noticeable sedimentation of the particles. As the layer thickness gradually decreases due to the water evaporation, the particle concentration increases with time. As the layer thins, the particles come closer and closer and often collide with each other, but no aggregation or irreversible particle attachment to the glass surface is noticed (Figure 3, top).

When the layer thickness becomes c.a. 10  $\mu\text{m}$ , one can see in reflected monochromatic light the appearance of Newton rings in the cell center (where the thickness is the smallest), which are a result from interference of the light reflected from the glass-water and water-air surfaces. After a certain time a plane-parallel wetting film with a thickness close to the particle diameter forms and spreads over an area of about 1  $\text{mm}^2$ . Still, the latex particles inside the layer continue to be involved in Brownian motion. Sometimes a few larger particles (a result of the polymerization procedure during the latex production) with diameters exceeding the mean film thickness can be seen in the film area. From the Newton rings which appear around each of these large particles, one sees that aqueous menisci form and, eventually, the tops of these particles can protrude from the water phase. No movement of these particles is noticed after that.

At a given moment a ring-shaped narrow zone of tightly packed particles is formed over the middle of the glass substrate. This is the onset of growth of a well-ordered array. The mean particle volume fraction in the water layer is lower than 10% at this moment. The ordered zone is encircled by a thicker and slightly concave meniscus. The particles located in the meniscus region begin to move toward the ordered zone, and upon reaching the boundary of the array they are incorporated into the ordered phase (Figure 3, bottom). Usually, the particles are ordered in domains with hexagonal packing. Thus, the front of the ordered domain advances with time in a radial direction from the center of the substrate toward the ring wall. Some of the particles firmly stick to the glass surface before reaching the ordered region (e.g., the three isolated

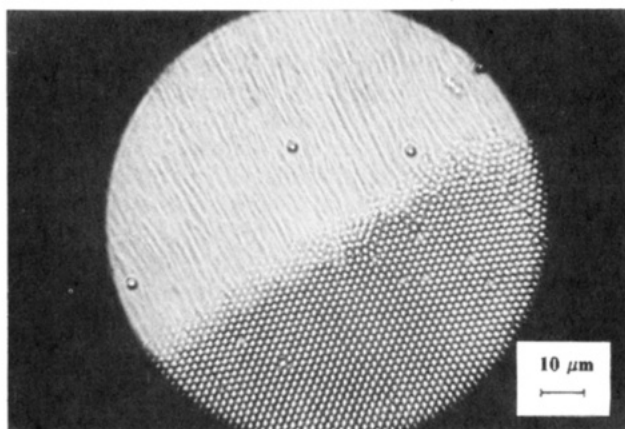
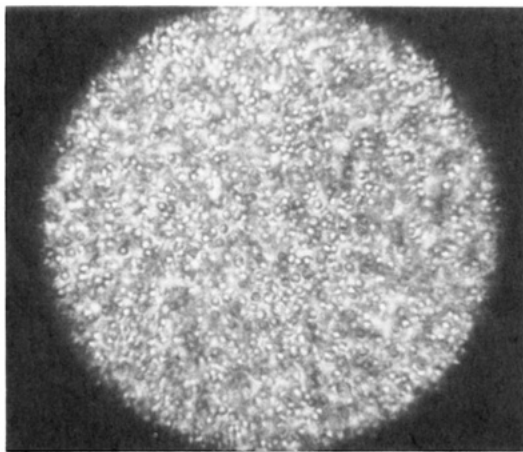


**Figure 3.** (Top) Concentrated latex particles in a water layer of thickness  $\sim 10 \mu\text{m}$ . (Bottom) Photograph of the process of ordering. The particles ("worms" in the upper left part of the photograph) are moving toward the ordered phase, building up the hexagonal array (lower right). Bar is equal to  $10 \mu\text{m}$ .

particles in the upper left part of Figure 3, bottom). After a certain time they are incorporated into the growing ordered monolayer but cause defects in the two-dimensional crystal. In reflected light one can see interference fringes in the encircling meniscus, which are close to the advancing border of the ordered region—Figure 4, top. From the distance between the fringes one can calculate that at the boundary of the array the meniscus has a slope below  $1^\circ$ . The thickness of the water layer gradually increases from the boundary of the ordered array toward the periphery of the cell.

Inside the ordered monolayer sometimes one can observe "lakes", e.g., regions free of particles, where the glass substrate is covered only by an aqueous layer. Interference fringes are observed in a vicinity of the shore of such a lake (Figure 4, bottom). The fringes show that the surface of the lake is concave: the thickness of the aqueous layer increases when approaching the particle monolayer. From the fringes one can estimate that the thickness of the aqueous layer at the boundary of the ordered array is slightly below  $1.7 \mu\text{m}$ .

When the radius of the ordered area becomes about 3–4 mm, one often observes a transition from monolayer to bilayer (Figure 5). Closer inspection through a high-magnification objective ( $\times 100$ ) shows that part of the particles reaching the boundary of the ordered phase rise over the first layer and form a second layer upon the first one. Besides, usually the boundary between the *hexagonal mono- and bilayers* consists of small domains of latexes ordered in a bilayer of particles packed in a *square lattice*

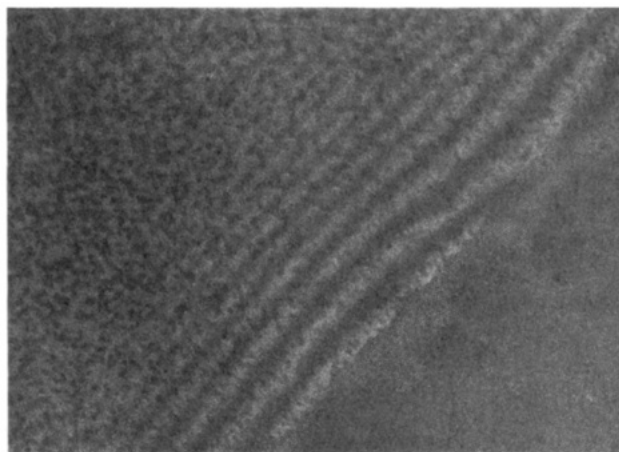


**Figure 4.** (Top) Interference pattern due to the slope of the liquid meniscus surrounding the ordered array (in the lower right zone). Every transition from a dark to bright band or vice versa corresponds to a 102-nm difference in the thickness of the liquid layer (low magnification). (Bottom) Interference pattern at the boundary between the ordered monolayer (the dark zone) and a "lake" (region free of particles where the substrate is covered only by a thin water layer—the bright zone) inside the array. The water layer thickness in the lake is below 50 nm, while at the boundary of the particle monolayer it is slightly below  $1.7 \mu\text{m}$ .

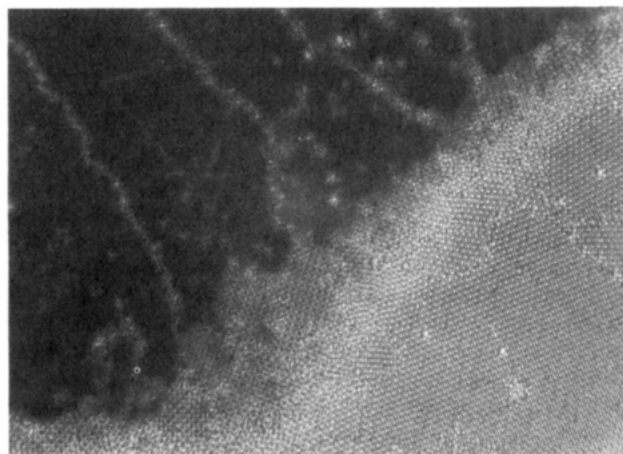


**Figure 5.** Transition between a monolayer (bright, lower right) and a bilayer (dark, upper left) of ordered particles. Particles packed in a square lattice can be seen in the transition zone.

(see Figure 5). In some experiments we observed formation of concentric ordered belts consisting of a periodically repeated hexagonal monolayer, square bilayer, and hexagonal bilayer.

**3.2. Factors Affecting the Array Formation.** In order to reveal the forces governing the ordering and to

explain the observed phenomena, we investigated the effect of different factors on the processes of array formation.

**Particle Size.** We performed a set of experiments with latex particles of smaller diameter: 0.81  $\mu\text{m}$ . The observed phenomena were very similar for the two suspensions of different sizes. The only difference worth mentioning is that the smaller particles moved faster during the stage of 2D crystal growth. The sequence of the observed phenomena and the final results seem to be qualitatively the same.

**Particle Concentration.** In a typical experiment like those described in the previous subsection, the volume (20  $\mu\text{L}$ ) and concentration (1 wt %) of the latex suspension have been chosen to provide (approximately) a dense monolayer of particles. In another set of experiments we have varied the latex concentration (keeping constant the overall volume of 20  $\mu\text{L}$ ) from 0.25 to 2.5 wt %. Although the concentration varied for over 1 order of magnitude, there is no substantial difference in the occurrence of the processes. One should notice only that when the particle concentration is higher, the area occupied by bilayers is larger. Oppositely, when the particle concentration is lower, large areas free of particles are formed between the parcels covered with a particle monolayer. Besides, in the latter case many particles stick to the glass surface before reaching the ordered regions and form many small groups consisting of several particles.

**Electrolyte Concentration.** The polystyrene latex particles in aqueous solution bear a negative surface electrical charge due to dissociation of surface ionizable groups. To study the role of the electrostatic interactions, we added  $\text{BaCl}_2$  (concentration  $5 \times 10^{-4}$  M) to the latex suspension. Since the  $\text{Ba}^{2+}$  ions partially adsorb at the particle surface, the magnitude of the surface potential decreases. The  $\zeta$ -potential changes from  $-106$  to  $-53$  mV. As a result, at the stage of Brownian motion a pronounced tendency for formation of transient aggregates (2–5 particles) is observed, which is certainly due to the screened electrostatic repulsion. This allows the attractive van der Waals interaction between the particles to become operative. The aggregation is reversible, and neither coagulation nor deposition onto the glass surface is observed. It turns out that, in spite of the decreased electrostatic repulsion, the process of ordering follows the same pattern. The only difference is that the rate of crystal formation is slightly slower. At a concentration of  $\text{BaCl}_2$  above  $2 \times 10^{-3}$  M, particle coagulation (formation of disordered three-dimensional aggregates) in the bulk of the suspension is observed and further water evaporation does not lead to two-dimensional crystallization.

The addition of 0.01 M NaCl also leads to suppression of the electrostatic repulsion and to reversible formation of transient aggregates in the bulk. The general trend of the observed processes is the same as without electrolyte. However, during the stage of ordering irreversible deposition of the latex particles onto the glass surface is often observed, and arrays consisting of smaller domains are obtained.

The fact that the addition of moderate concentrations of electrolyte changed significantly the  $\zeta$ -potential without affecting the general occurrence of the phenomenon suggests that neither electrostatic repulsion nor van der Waals attraction between the particles is the driving force of the two-dimensional crystallization. Hence, there should be another source of interaction between the particles. Such a source is discussed in section 3.3 below.

**Water Evaporation Rate.** As described above, the 2D crystal growth takes place through a directional motion

of particles from the disordered phase toward the ordered one. The simplest way to investigate the role of the water evaporation on this process is to change the evaporation rate. For this purpose the glass cover (7 in Figure 2) was replaced by a plane-parallel glass plate situated right on the top of the brass plate (4). Thus, the volume of the air space above the suspension was reduced from c.a. 250 to 1  $\text{cm}^3$ . This resulted in a strong decrease (about 1 order of magnitude) of the rate of all processes, including the speed of directional motion of the particles and the rate of array growth. Moreover, very large and well-ordered domains were obtained, and comparatively larger parts of the substrate were covered with bilayers. Even trilayers were observed in some regions. These experiments demonstrate the important role of the water evaporation on the ordering. We made use of this strong influence of the evaporation rate to obtain domains consisting of bilayers, trilayers, tetralayers, etc., in a controlled way; see section 3.4 below.

**Presence of Surfactants.** It is known that the surfactant solutions exhibit a slower evaporation rate than pure water at the same conditions.<sup>20</sup> We investigated the effect of two types of surfactants (anionic sodium dodecyl sulfate (SDS) and cationic hexadecyltrimethylammonium bromide (HTAB)) on the dynamics of ordering.

HTAB in a concentration of  $10^{-4}$  M (which is 9 times below the critical micelle concentration) reduced by about 1 order of magnitude the speed of the directional particle motion and the rate of the 2D crystal growth during the stage of array formation. Large and well-ordered domains were obtained in these experiments. The increase of the surfactant concentration leads to deposition of many particles on the glass surface before their incorporation in the array, which causes dislocations and other defects in the 2D crystal. Probably, this is due to the adsorption of positively charged surfactant molecules on the negatively charged particle and glass surfaces, which suppresses the electrostatic repulsion between them. At even higher surfactant concentrations ( $\sim 10^{-3}$  M), the particles coagulate in the bulk suspension and further water evaporation does not lead to 2D crystallization.

The addition of  $8 \times 10^{-3}$  M SDS to the latex suspension also slowed the dynamics of ordering. Neither particle deposition on the substrate nor coagulation was observed, and well-ordered arrays were obtained in this case. It is worth mentioning that in areas with low coverage of particles the ordering takes place through a peculiar rearrangement of the particles when the layer thickness becomes approximately equal to the particle diameter. Narrow well-ordered domains are formed, which surround large areas free of particles; see Figure 6. Most probably, the specific structure of the monolayer shown in Figure 6 is due to the capillary meniscus forces acting between the particles (see below).

**Shape of the Liquid Surface.** In the experiments described above the ordering starts from the central (thinner) part of the slightly concave liquid layer containing the latex particles. To provide this shape of the meniscus, the edge of the Teflon ring (3 in Figure 2), which is in contact with the glass substrate, must be cut slantwise as shown in the inset of Figure 2. This specific shape of the ring allows wetting of the ring walls by the suspension and formation of a concave air–water surface. Alternatively, if the inner wall of the ring is made exactly vertical, the suspension does not wet the wall (the three-phase contact

(20) Davies, J. T.; Rideal, E. K. *Interfacial Phenomena*, 2nd ed.; Academic Press: New York, 1963; Chapter 7.

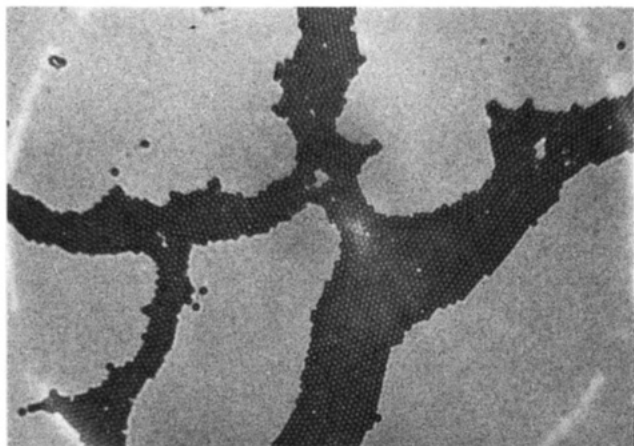


Figure 6. Ordered domains of particles at a low particle concentration obtained in the presence of  $8 \times 10^{-3}$  M SDS.

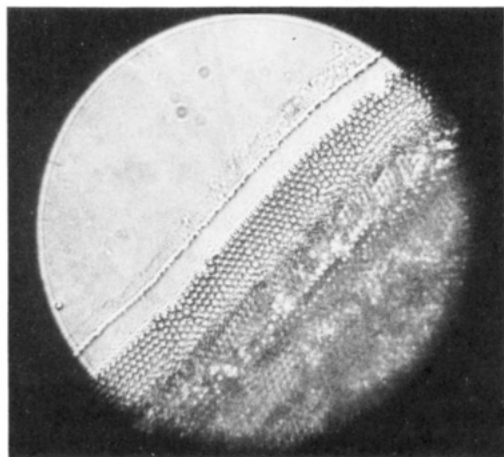


Figure 7. Periphery of a latex drop drying on a glass plate without a surrounding ring. A thick multilayer of latex deposits is formed (lower right zone).

angle air-water-Teflon is known<sup>21</sup> to be slightly above  $90^\circ$ ) and a convex air-water surface forms. In this case the ordering starts somewhere at the periphery of the layer in close vicinity to the ring wall. Again a directional motion is observed from the disordered toward the ordered regions. The final ordered array obtained in this regime consists of smaller domains with a lot of defects.

We have performed several experiments with a suspension drop placed at a glass plate without a surrounding ring. The drop spreads over a certain area and forms a convex surface which meets the glass at a contact angle of a few degrees. A thick multilayer of particles accumulates at the drop periphery as a result of the directional motion of the particles from the center of the drop toward its boundary during the evaporation of the water; see Figure 7. In the central part only a small amount of particles remains and forms small clusters. Large and well-ordered arrays were not obtained in this way.

The general conclusion from these experiments is that the overall shape of the liquid surface is quite important for the array formation and for the quality of the obtained 2D crystals.

**"Impurities" of Large Particles.** In some cases a much larger particle can be present in the suspension. When the advancing front of the ordered array approaches such a particle, one observes distortion of the interference fringes at the border between the meniscus and the crystal.

(21) Janczuk, B.; Bialopiotrowicz, T. *J. Colloid Interface Sci.* 1990, 140, 362.

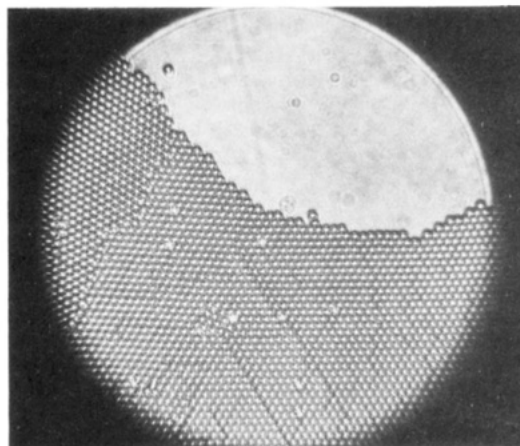


Figure 8. A transition from an ordered monolayer array to an area free of particles.

From the shape of the interference fringes one can conclude that the water layer is thicker in the vicinity of the large particle. As a result the smaller particles carried by the water flux (see below) "fill up" the conical space below the air-water surface formed around the larger particle. Belts with consecutively increasing numbers of layers from the periphery toward the center of this cone are observed. One can follow the transitions from monolayer to bilayer, trilayer, etc. of hexagonally packed particles. At the boundaries between the regions with different numbers of layers, usually one sees small domains of square-packed particles; see section 3.4.

**3.3. Mechanism of 2D Array Formation from Micrometer-Size Latex Particles.** It is generally accepted that the formation and behavior of 3D colloidal crystals are controlled by the repulsive electrostatic forces acting between the particles.<sup>6-13,22,23</sup> However, the results reported above indicate that some other type of interactions should be considered as responsible for the 2D array formation. Indeed, the addition of electrolytes ( $\text{BaCl}_2$  or  $\text{NaCl}$ ) strongly suppresses the electrostatic repulsion without substantial changing of the ordering processes. Similarly, the change of the concentration of the latex particles does not affect the onset of the ordering, whereas with 3D crystals this is the major factor governing the phase transitions. In all cases the array formation starts when the thickness of the water layer becomes approximately equal to the particle diameter and the crystal growth takes place through a directional motion of particles toward the ordered regions. A coexistence between well-ordered domains and regions free of particles is often observed (see Figure 8). The last two experimental facts, in particular, cannot be explained by the action of repulsive forces alone.

Considering all of our experimental observations, we propose the following two-stage mechanism of the array formation. At the first stage a "nucleus" of ordered phase appears when the upper surface of the thinning aqueous layer in the wetting film presses the latex particles toward the water-glass interface. As shown theoretically by Kralchevsky et al.<sup>24-26</sup> when spherical particles are partially

(22) Chaikin, P. M.; Pincus, P.; Alexander, S.; Hone, D. *J. Colloid Interface Sci.* 1982, 89, 555.

(23) Voegtli, L. P.; Zukoski, C. F., IV *J. Colloid Interface Sci.* 1991, 141, 79.

(24) Kralchevsky, P. A.; Paunov, V. N.; Ivanov, I. B.; Nagayama, K. *J. Colloid Interface Sci.* 1992, 151, 79.

(25) Kralchevsky, P. A.; Paunov, V. N.; Denkov, N. D.; Ivanov, I. B.; Nagayama, K. *J. Colloid Interface Sci.*, in press.

(26) Paunov, V. N.; Kralchevsky, P. A.; Denkov, N. D.; Nagayama, K. *J. Colloid Interface Sci.*, in press.

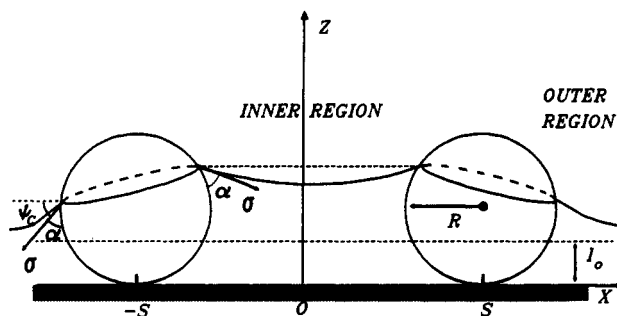


Figure 9. Two spheres partially immersed in a liquid layer on a horizontal solid substrate. The deformation of the liquid meniscus gives rise to interparticle attraction (see the text).

immersed in a liquid layer on a horizontal solid substrate, the deformations of the liquid-gas interface give rise to strong and long-range interparticle capillary forces. The physical nature of these forces can be explained as follows. Let us consider two particles of radius  $R$ , partially immersed in a liquid layer, whose thickness tends to a constant value  $l_0$  at a large distance from the two particles (see Figure 9). The shape of the meniscus obeys the Laplace equation of capillarity and is determined by the distance  $L = 2s$  between the particles, the layer thickness  $l_0$ , and the value of the contact angle  $\alpha$ , which characterizes the particle wettability. The water level in the inner region (between the particles) is higher than in the outer region. The ensuing inclination of the three-phase contact lines at the particle surfaces gives rise to two capillary effects, both leading to attraction: (i) *pressure effect*, caused by the higher hydrostatic pressure in the gas phase than the pressure in the liquid at  $z > l_0$  (especially in the inner region), this pressure difference pushes the particles toward each other; (ii) *surface force effect* due to the fact that the slope (with respect to the horizontal) of the liquid surface, and hence the  $x$  component  $\sigma_x$  of the surface tension force  $\sigma$ , varies along the contact line. The developed theory<sup>24-26</sup> shows that for micrometer-size and smaller particles the surface tension effect exceeds the pressure effect by many orders of magnitude. With high accuracy the attractive capillary force (more precisely its horizontal projection  $F_x$ ) can be expressed as<sup>25</sup>

$$F_x \approx 2\pi\sigma r_c^2 (\sin^2 \Psi_c) (1/L) \quad r_c \ll L \ll (\sigma/(\Delta\rho)g)^{1/2} \quad (1)$$

where  $\sigma$  is the surface tension of the liquid,  $r_c$  is the radius of the three-phase contact line at the particle surface,  $\Psi_c$  is the mean meniscus slope angle at the contact line,  $g$  is the gravitational acceleration, and  $\Delta\rho$  is the difference between the mass densities of the liquid and gas phases.

It is worth noting that the capillary forces between particles partially immersed in a liquid layer on a solid substrate (we call them "immersion capillary forces"<sup>26</sup>) are many orders of magnitude greater than the capillary forces between similar particles floating attached to a single interface,<sup>26-28</sup> which are sometimes called "flotation capillary forces". It was established<sup>24-26</sup> that the immersion forces are so strong that the respective energy of capillary attraction can be much larger than the thermal energy,  $k_B T$ , even with submicrometer particles. On the contrary, the flotation forces are negligible for particles smaller than c.a.  $10 \mu\text{m}$ . This is demonstrated in Figure 10 where the two types of capillary interaction are compared for a wide range of particle sizes. The other parameters are particle mass density  $\rho_p = 1.05 \text{ g/cm}^3$ ,  $\sigma = 72 \text{ mN/m}$ ,  $\alpha = 30^\circ$ ,  $L$

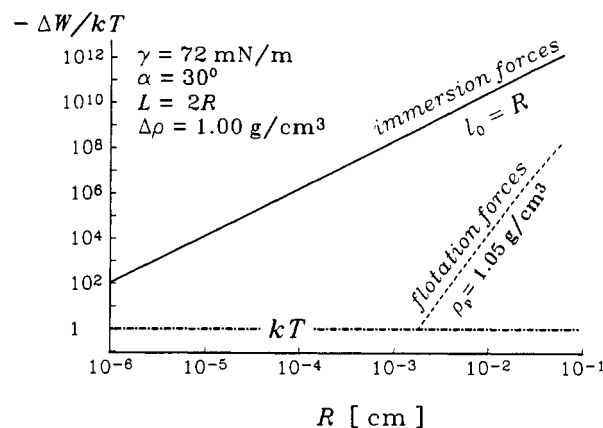


Figure 10. Comparison between immersion<sup>24,25</sup> and flotation<sup>26,28</sup> capillary forces: dependence of the capillary interaction energy,  $\Delta W$ , on the particle radius,  $R$ . The full curve is calculated by using eq 4.11 from ref 24, and the dashed curve is calculated by using eq 4.7 from ref 26.

$= 2R$ , and  $l_0 = R$ . The drastic difference between the two types of capillary forces is due to the different deformation of the water-air interface, which in turn is determined by the force exerted on the three-phase contact line. The small floating particles are too light to create substantial deformation of the liquid surface. In the case of immersion forces the particles are restricted in the vertical direction by the solid substrate. Then, as the film becomes thinner, the liquid surface deformation increases, thus giving rise to a strong interparticle attraction. The deformation in this case is much larger (the angle  $\Psi_c$  in eq 1 is orders of magnitude greater) than the one caused by the particle weight for similar floating particles.<sup>26</sup> In our experiments the capillary interaction is determined by immersion forces, while in the experiments on particle aggregation on a water surface performed previously<sup>29,30</sup> the flotation type forces were operative.

Once the nucleus is formed, the second stage of crystal growth starts through directional motion of particles toward the ordered array. The horizontal component of the capillary forces could be a reason for this motion: the particles in the ordered phase attract the nearest ones, causing a flux directed toward the ordered regions. However, this hypothesis cannot explain some experimental observations. For example, as mentioned earlier, the ordered particle monolayer is encircled by a concave liquid layer, whose thickness is larger than the particle diameter. The moving particles are totally immersed in the liquid layer, and hence, they are not subjected to the action of capillary forces. The formation of bilayers also cannot be explained by the action of the capillary force alone, because the particles in the bottom layer are totally immersed in the water. Our observations suggest that the directional particle motion is caused by a convective water flux which carries along the particles toward the ordered phase. The reason for the appearance of such a convective flux can be explained in the following way. The evaporation of water leads to a gradual decrease of the liquid layer thickness with time. Until the thickness is larger than the particle diameter, it decreases uniformly. Once ordered regions are formed, the thinning of the water layer inside them is slowed due to the hydrophilicity of the particles. Indeed, the evaporation from the concave menisci between the particles, clustered in a nucleus, must increase the local curvature and hence the local sucking

(27) Nicolson, M. M. *Proc. Cambridge Philos. Soc.* 1949, 45, 288.

(28) Chan, D. Y. C.; Henry, J. D.; White, L. R. *J. Colloid Interface Sci.* 1981, 79, 410.

(29) Allain, C.; Joughier, B. *J. Phys. (Paris), Lett.* 1983, 44, L-421.

(30) Camoin, C.; Blanc, R. *J. Phys. (Paris), Lett.* 1985, 46, L-67.

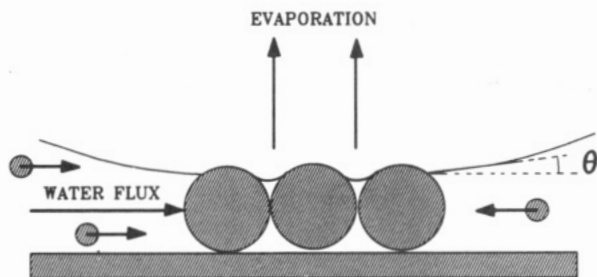


**Figure 11.** Convective flux toward the ordered phase due to the water evaporation from the menisci between the particles in the 2D array.

capillary pressure. This brings about an intensive water influx from the thicker parts of the layer where the pressure is higher. The convective influx carries along the suspended particles toward the clusters (Figure 11). The "newcomers" remain attached to the domains, pressed by the hydrodynamic pressure of the water and captured by the capillary attraction.

We carried out additional experiments to verify the proposed mechanism by using mixtures of particles of diameters 1.70 and 0.81  $\mu\text{m}$ . By controlled water evaporation (see below) a water film of thickness intermediate between the diameters of the two kinds of particles was obtained. Under these conditions menisci are formed around each larger particle. The vertical component of the surface tension force,  $F_z = 2\pi\sigma r_c \sin \Psi_c$ , presses these particles against the glass surface. When this force becomes large enough, the bigger particles are immobilized (due to the friction with the glass) before they have reached the already existing ordered clusters. However, the smaller particles still move inside the water layer and are carried by convection toward the clusters (Figure 11).

By decreasing or increasing the water evaporation rate we were able, respectively, to speed up or slow down the convective transport of the small particles. In agreement with the proposed mechanism, this effect can be explained by the change of curvature of the liquid menisci between the particles in the nucleus (see Figure 11). For instance, the increased evaporation decreases the level of the water between the particles and increases the curvature of the menisci, thus rising the local sucking capillary pressure which drives the water influx toward the nucleus. In the opposite case when the level of the water between the particles is increased because of water condensation (due to some increase of the humidity of the gas inside the cell), the sucking pressure is decreased and one observes a decrease of the particle convective influx. A further increase of the humidity leads to complete stopping of the process of ordering and even to disintegration of the ordered clusters and restoration of the chaotic particle motion.

The proposed mechanism is also in agreement with the results about the effect of the other investigated factors. For example, from this viewpoint it is clear why electrolytes (in moderate concentrations) do not influence the ordering; the electrostatic interactions play a secondary role (if any) in these processes.

#### 3.4. Methods for Controlling the Array Formation.

The mechanism described above suggests at least two ways for control of the ordering process: (i) control of the speed of the convective flow by changing the rate of water evaporation; (ii) control of the profile of the liquid meniscus encircling the ordered array by ejecting (injecting) some amount of suspension during the experiment. Both ways lead to a change of the liquid layer thickness and of the

surface slope at the boundary between the array and the encircling meniscus.

For controlling the process of ordering a modified experimental cell was used. By changing the temperature of the upper glass cover of the cell we have the possibility to vary the relative water humidity above the suspension layer and thus to speed up (or slow down) the water evaporation from the layer. On the other hand, the injection (or sucking out) of suspension into (from) the cell leads to an increase (decrease) of the suspension volume, thus changing the shape of the liquid meniscus. As a rule, 2D arrays of better quality (larger "monocrystal" domains) are obtained when the rate of 2D crystal growth is lower.

The result of the ordering process turns out to be connected also with the magnitude of the angle  $\theta$  characterizing the slope of the encircling liquid meniscus at the boundary with the growing 2D array; see Figure 11. Since the liquid layer inside the cell is concave (see Figure 2), the meniscus slope is larger close to the inner cylindrical wall of the cell. That is why, when the ordered particle monolayer in the middle of the substrate is growing toward the cylindrical wall, the angle  $\theta$  gradually increases. The magnitude of  $\theta$  can be estimated at every moment from the interference fringes (Figure 4, top). When  $\theta$  becomes large enough, one observes formation of an ordered bilayer, instead of a monolayer. The angle  $\theta$  can be varied either by changing of the water evaporation rate or by changing the suspension volume in the cell. For example, the accelerated water evaporation and the ejection of suspension from the meniscus lead to a decrease of  $\theta$ . Thus, they can suppress the formation of a bilayer and other multilayers. In the opposite case, under a controlled increase of the angle  $\theta$  (via slowed evaporation or injection of a suspension into the cell) one can promote formation of ordered multilayers of different thickness.

Closer inspection of the multilayers with a higher magnification objective ( $\times 100$ ) shows that they consist of well-ordered domains of hexagonally packed particles. The higher magnification reveals also that the narrow bands between these layers consist of many small domains of square-packed particles, like those shown in Figure 5. The overall sequence of layers is the following: 1 $\Delta$ , 2 $\square$ , 2 $\Delta$ , 3 $\square$ , 3 $\Delta$ , ..., where the number denotes the number of layers and the symbols mean hexagonal ( $\Delta$ ) or square ( $\square$ ) packing of the particles. The observed trend exactly coincides with the phase diagram for the system of spheres confined in a narrow slit of thickness comparable with (but larger than) the particle diameter, theoretically calculated and experimentally observed by Pieranski et al.<sup>2,3</sup> This means that, in spite of the nonequilibrium dynamic character of the observed phenomenon, the number of layers and the kind of packing are determined by the thickness of the liquid layer, just like in the experiments of Pieranski, as long as there are enough particles to fill in the accessible space.

#### 4. Concluding Remarks

The main results from this experimental study can be summarized as follows. A simple experimental cell was designed which allows direct microscopic observation of the dynamics of two-dimensional array formation from micrometer-size latex particles; see Figure 2. The experiments show that the onset of the ordering process coincides with the moment when the thickness of the liquid layer containing the particles becomes smaller than the particle diameter. The deformation of the liquid meniscus around the protruding tops of the particles gives rise to inter-

particle attraction. In the very beginning closely situated particles in the film form clusters—two-dimensional nuclei of the ordered array, which trigger further growth of the ordered domains by convective transport of particles toward the ordered region—Figure 3, bottom. This transport is caused by water evaporation from the menisci between the particles in the clusters, which increases the local capillary pressure sucking the liquid into the clusters (see Figure 11).

The rate of water evaporation and the shape of the air-water surface affect considerably the type and quality of the obtained arrays. Well-ordered multilayered domains (up to eight layers) have been obtained by controlling the water evaporation and the meniscus shape. The proposed mechanism explains why a variation of the particle

concentration and the presence of electrolyte (in moderate concentrations) do not affect significantly the process. It is worth noting in this respect that, in contrast with the crystal formation in bulk suspension, the process of two-dimensional ordering, observed by us, is driven by capillary meniscus phenomena.

**Acknowledgment.** This work was supported by the Research and Developmental Corp. of Japan (JRDC) under the Program “Exploratory Research for Advanced Technology” (ERATO). The calculations and drawing of Figures 9 and 10 by V. N. Paunov are acknowledged.

**Registry No.** Polystyrene, 9003-53-6; sodium dodecyl sulfate, 151-21-3; hexadecyltrimethylammonium bromide, 57-09-0.